

# Policy Regularization with Noisy Advantage Values for Cooperative Multi-agent Actor-Critic methods

Siyue Hu\*

National Taiwan University  
Taipei, Taiwan  
husiyuehusiyue@gmail.com

Weixun Wang

Tianjin University  
Tianjin, China Mainland  
wxwang@tju.edu.cn

Jian Hu\*\*

National Taiwan University  
Taipei, Taiwan  
r08944053@ntu.edu.tw

Shih-wei Liao

National Taiwan University  
Taipei, Taiwan  
liao24@gmail.com

## ABSTRACT

Multi-Agent Reinforcement Learning (MARL) has seen revolutionary breakthroughs with its successful application to multi-agent cooperative tasks such as robot swarms control, autonomous vehicle coordination, and computer games. Recent works have applied the Proximal Policy Optimization (PPO) to the multi-agent tasks, called Multi-agent PPO (MAPPO). However, previous literature shows that the vanilla MAPPO with a shared value function may not perform as well as Independent PPO (IPPO) and the finetuned QMIX. Thus MAPPO-agent-specific (MAPPO-AS) further improves the performance of vanilla MAPPO and IPPO by the artificial agent-specific features. In addition, there is no literature that gives a theoretical analysis of the working mechanism of MAPPO. In this paper, we firstly theoretically generalize single-agent PPO to the vanilla MAPPO, which shows that the vanilla MAPPO is approximately equivalent to optimizing a multi-agent joint policy with the original PPO. Secondly, we find that vanilla MAPPO faces the problem of *The Policies Overfitting in Multi-agent Cooperation (POMAC)* as they learn policies by the sampled centralized advantage values. Then POMAC may lead to updating the policies of some agents in a suboptimal direction and prevent the agents from exploring better trajectories. To solve the POMAC problem, we propose a novel policy regularization method, i.e, Noisy-MAPPO and Advantage-Noisy-MAPPO, which smooth out the advantage values by noise. The experimental results show that the average performance of Noisy-MAPPO is better than that of finetuned QMIX and MAPPO-AS, and is much better than the vanilla MAPPO. We open-source the code at <https://github.com/hijkzzz/noisy-mappo>.

## KEYWORDS

Multi-agent, Reinforcement Learning, Noise, PPO

### ACM Reference Format:

Siyue Hu\*, Jian Hu\*\*, Weixun Wang, and Shih-wei Liao. 2022. Policy Regularization with Noisy Advantage Values for Cooperative Multi-agent Actor-Critic methods. In *preprint*, , IFAAMAS, 13 pages.

\* Jian Hu and Siyue Hu contributed equally to this work.

\*\* Corresponding Author.

## 1 INTRODUCTION

Multi-Agent Reinforcement Learning (MARL) has seen revolutionary breakthroughs with its successful application to multi-agent cooperative tasks such as robot swarms control [9], autonomous vehicle coordination [2] and computer games [24]. As for scalability and communication security problems, decentralized execution of multi-agent policies that act only on their local observations is widely used. An intuitive approach for decentralized multi-agent policy learning is the Independent Q Learning (IQL) [29]. However, IQL does not address the non-stationarity introduced due to the changing policies of the learning agents. Thus, unlike single-agent Reinforcement Learning (RL) algorithms, there is no guarantee of convergence even at the limit of infinite exploration. Therefore, the *Centralized Training and Decentralized Execution (CTDE)* [13], which allows for agent to access global information during training stage, is widely used in MARL algorithms [16, 23].

Many CTDE algorithms, e.g. MADDPG [16], MAAC [10], QMIX [23] and Qatten [32], have been proposed for multi-agent cooperative tasks. Among these algorithms, the finetuned QMIX [8] achieves the SOTA performance in the popular MARL benchmark environment Starcraft Multi-Agent Challenge (SMAC) [24]. To enable effective CTDE for multi-agent Q-learning, the Individual-Global-Max (IGM) principle [27] of equivalence of joint greedy action and individual greedy actions is critical. QMIX ensures that the IGM condition holds by the mixing network with *Monotonicity Constraint* [23]. However, the mixing network leads to limitations in its scalability, and monotonicity constraints prevent it from learning correctly in non-monotonic environments [27]. We turn our attention to the efficient single-agent RL algorithms, such as Trust Region Policy Optimization (TRPO) [25] and Proximal Policy Optimization (PPO) [26], as their unlimited expressive power and high sample efficiency. Recently, [1, 4, 33] have applied the PPO to the multi-agent tasks, called Multi-agent PPO (MAPPO); and [14] proposed a multi-agent TRPO algorithm, but only for the case where each agent has a private reward.

The literature [4] shows that vanilla MAPPO with centralized value function may not perform as well as Independent PPO (IPPO), and literature [33] further improves the performance of vanilla MAPPO and IPPO by artificial agent-specific features, called MAPPO-agent-specific (MAPPO-AS) (details in Sec. 6). In addition, there is no literature that gives a theoretical analysis for the working mechanism of PPO in multi-agent settings. By contrast, we find that

vanilla MAPPO faces the problem of *The Policies Overfitting in Multi-agent Cooperation*(POMAC) as they learn policies by the sampled centralized advantage values [18]. Then POMAC may lead to updating the policies of some agents in a suboptimal direction and prevent the agents from exploring better trajectories.

In this paper, (1) We extend single-agent PG and PPO to Multi-agent PG (MAPG) and Multi-agent PPO (MAPPO) from a theoretical perspective, which shows that MAPPO is equivalent to optimizing a multi-agent joint policy with the single-agent PPO approximately. (2) Inspired by the label smoothing technique [22, 31], we propose a novel policy regularization methods, i.e, Noisy-MAPPO and Advantage-Noisy-MAPPO, which smooth out the advantage values by noise to solve the POMAC problem. (3) Empirical results show that our approach achieves better performance than fine-tuned QMIX [8], MAPPO-AS in previous work [33], and is much better than the vanilla MAPPO (Sec. 5 and Appendix C.1), without scalability, expressiveness limitations, and artificial agent-specific features.

*We are the first to propose to improve the effectiveness of the Multi-agent Actor-Critic algorithms by policies regularization with noisy advantage values.*

## 2 BACKGROUND

**Dec-POMDP** We consider a cooperative task, which can be described as a decentralized partially observable Markov decision process (Dec-POMDP)[20]. The cooperative agent chooses sequential actions under partial observation and environment stochasticity. Dec-POMDP is a tuple  $(\mathcal{S}, \mathcal{A}, \mathcal{O}, \mathcal{R}, \mathcal{P}, n, \gamma)$  where  $\mathcal{S}$  is state space.  $\mathcal{A}$  is joint action space.  $o_i = \mathcal{O}(s; i)$  is partially observation for agent  $i$  at global state  $s$ .  $\mathcal{P}(s'|s, \mathcal{A})$  is the state transition probability in the environment given the joint action  $\mathcal{A} = (a_1, \dots, a_N)$ . Every agent has same shared reward function  $\mathcal{R}(s, \mathcal{A})$ .  $N$  denotes the number of agents and  $\gamma \in [0, 1)$  is the discount factor. The team of agents attempt to learn a joint policy  $\pi = \langle \pi_1, \dots, \pi_N \rangle$  that maximises their expected discounted return.

$$V^\pi(s_0) = \mathbb{E}_{a^1 \sim \pi^1, \dots, a^N \sim \pi^N, s \sim T} \left[ \sum_{t=0}^{\infty} \gamma^t r_t(s_t, a_t^1, \dots, a_t^N) \right] \quad (1)$$

**CTDE** Centralized training with decentralized execution(CTDE) paradigm[13], in which agents can obtain additional information and centralized joint learning; while in the testing phase, agents make the decision based on their own partially observation. Next, we introduce some CTDE algorithms for the multi-agent credit assignment [3].

**Credit assignment** Multi-agent credit assignment [3] is a critical challenge: in cooperative settings, joint actions typically generate only global rewards, making it difficult for each agent to deduce its own contribution to the team's success. Many CTDE algorithms have been proposed to solve this problem: COMA [5] trains decentralized agents by a centralized critic with counterfactual advantages. MADDPG [16] and MAAC [10] trains a joint critic to extend DDPG [15] to the multi-agent setting, which can be seen as implicit credit assignment [34]. VDN [28], QMIX [23] and Qatten [32] decompose the joint action-value function to individual action-value functions by the Q value mixing networks.

**QMIX** Then, we introduce QMIX in detail as it often used as a baseline in MARL. QMIX [23] proposes a value decomposition network that decomposes  $Q_{tot}$  into  $Q_i$  (Eq. 2), corresponding to the utilities of each agent  $i \in N$ , based on monotonicity constraints (Eq. 3),

$$Q_{tot}(s, \mathbf{a}; \theta, \phi) = g_\phi \left( s, Q_1(\tau^1, a^1; \theta^1), \dots, Q_N(\tau^N, a^N; \theta^N) \right) \quad (2)$$

$$\frac{\partial Q_{tot}(s, \mathbf{a}; \theta, \phi)}{\partial Q_i(\tau^i, a^i; \theta^i)} \geq 0, \quad \forall i \in N \quad (3)$$

The constraints Eq. 3 ensure that the greedy actions of each agent  $Q_i$  are consistent with that of  $Q_{tot}$ . QMIX assigns rewards to each agent through learnable mixing networks  $\phi$ . However, the monotonicity constraints limit the expressive power of QMIX, which may learn error argmax action in nonmonotonic cases [27] [17]. Besides, we consider a task including millions of agents, but only several states, the mixing network faces the problem of explosion in the size of  $Q_i$ .

## 3 MULTI-AGENT ACTOR-CRITIC

In this section, we first introduce the single-agent policy-gradient algorithms and discuss the non-stationary problems in multi-agent settings. Then, we extend the single-agent policy-gradient to multi-agent policy-gradient from the theoretical perspective, which shows that **the vanilla MAPPO is approximately equivalent to optimizing a independent joint policy with PPO.**

### 3.1 Single-agent

**Policy Gradient (PG)** In the on-policy case, the gradient of the object value function  $V^\pi(s_0) \stackrel{\text{def}}{=} \mathbb{E}_\pi \left[ \sum_{t \geq 0} \gamma^t r_t \right]$ , where  $\gamma \in [0, 1)$  with respect to some parameter of the policy  $\pi$  is

$$\nabla V^\pi(s_0) = \mathbb{E}_\pi \left[ \sum_{t \geq 0} \gamma^t \nabla \log \pi(a_t | s_t) A^\pi(s_t, a_t) \right] \quad (4)$$

where  $A^\pi(s_t, a_t) := Q^\pi(s_t, a_t) - V^\pi(s_t)$  is the advantage value function [18] of policy  $\pi$ , where  $Q^\pi(s_t, a_t) := r_t + \gamma V^\pi(s_{t+1})$  is the state action value function. Intuitively, PG makes the policy  $\pi$  closer to the actions with large advantage value by gradient ascending.

**Proximal Policy Optimization (PPO)** [26] [25] aims to maximize the objective function  $V^\pi(s_0)$  subject to, trust region constraint which enforces the distance between old and new policies measured by KL-divergence to be small enough, within a parameter  $\delta$ ,

$$J^{PPO} = \mathbb{E}_{a_t, s_t \sim \pi_{old}} \left[ \frac{\pi(a_t | s_t)}{\pi_{old}(a_t | s_t)} A^{\pi_{old}}(s_t, a_t) \right] \quad (5)$$

where  $\frac{\pi(a_t | s_t)}{\pi_{old}(a_t | s_t)}$  is the Importance sampling (IS) weight, with KL-divergence constraint,

$$\mathbb{E}_{s \sim \rho^{\pi_{old}}} \left[ D_{KL}(\pi_{\theta_{old}}(\cdot | s) \parallel \pi_{\theta}(\cdot | s)) \right] \leq \delta \quad (6)$$

where  $\rho^{\pi_{old}}$  is the discounted state distribution [25] sampled by policy  $\pi_{old}$ . [25] prove that  $J^{PPO}$  is equivalent to the Natural Policy Gradient (NPG) [11], which enable the the gradient in the steepest

direction of object function. However, in large-scale neural networks, the KL-divergence constraint causes the objective function to be difficult to solve. Therefore, PPO proposes an approximate objective function (Eq. 8),

$$r = \frac{\pi(a | s)}{\pi_{\text{old}}(a | s)} \quad (7)$$

$$J^{\text{PPO2}} = \mathbb{E}_{a_t, s_t \sim \pi_{\text{old}}} \left[ \min \left( r A^{\text{old}}(s, a), \text{clip}(r, 1 - \epsilon, 1 + \epsilon) A^{\text{old}}(s, a) \right) \right] \quad (8)$$

The function  $\text{clip}(r, 1 - \epsilon, 1 + \epsilon)$  clips the ratio to be no more than  $1 - \epsilon$  and no less than  $1 + \epsilon$ , which approximates the KL-divergence constraint.

### 3.2 Multi-agent

**Non-stationary Problem** However, applying these single-agent RL algorithms to the multi-agent faces the problem of environmental non-stationarity. For a certain agent  $i$  in a multi-agent system, we can treat other agents' policies as part of the environment; then, the Bellman Equation is

$$V^{\pi^i}(s) = \sum_a \pi^i(a^i | s) \sum_{s', r} p(s', r | s, a^i, \vec{\pi}^-) (r + v_{\pi^i}(s')) \quad (9)$$

where  $p(s', r | s, a, \vec{\pi}^-)$  is the state transition function in the multi-agent setting, and  $\vec{\pi}^-$  denotes the policies of other agents. Since the policy of each agent is updated synchronously, the state transition function  $p$  is non-stationary, and thus the convergence of the Bellman Equation cannot be guaranteed.

**Joint Policy Modeling** To solve above non-stationary problem, we model all agents' policies as a joint policy. i.e., we consider the autoregressive joint policy with  $N$  agents, likewise COMA [5],

$$\begin{aligned} \pi(\vec{a} | s) &= \prod_i \pi^i(a^i | s, a^{<i}) \\ &\approx \prod_i \pi^i(a^i | s) \end{aligned} \quad (10)$$

$$\approx \prod_i \pi^i(a^i | \tau^i) \quad (11)$$

If the agent **can infer the actions of other agents** from global state  $s$ , then Eq. 10 holds equivalently. We note that all sub-policies depend on the same state  $s$ , so they are not completely independent. If actions and observations history  $\tau^i$  contains enough information for right decisions, i.e., the agent can infer the actions of other agents and other information it needs through  $\tau^i$ , the above Eq. 11 holds equivalently. This joint policy treats all agents as a super-agent, thus avoids introducing other agents' policies in the state transition function  $p$ , in effect obviating the non-stationary.

**Multi-agent PG (MAPG)** Then, we put the Eq. 11 into Eq. 4 to simplify the PG formula,

$$\begin{aligned} g &= \mathbb{E}_{a_t, s_t \sim \pi} [\nabla \log \pi(\vec{a}_t | s_t) A(s_t, \vec{a}_t)] \\ &\approx \mathbb{E}_{a_t, s_t \sim \pi} \left[ \nabla \log \prod_i \pi^i(a_t^i | \tau_t^i) A(s_t, \vec{a}_t) \right] \\ &= \sum_i \mathbb{E}_{a_t, s_t \sim \pi} [\nabla \log \pi^i(a_t^i | \tau_t^i) A(s_t, \vec{a}_t)] \end{aligned} \quad (12)$$

Eq. 12 shows that we can optimize the decentralized policies using the single-agent PG gradient, with a centralized advantage function. This implies that we use the shared centralized advantage values as

$$A^\pi(s_t, a_t) = r_t + \gamma V^\pi(s_{t+1}) - V^\pi(s_t) \quad (13)$$

and fortunately, CTDE allows us to train a central value function using global information  $s$ .

**Multi-agent PPO (MAPPO)** Intuitively, we can directly use the PPO (Eq. 8) to optimize the multi-agent joint policy (Eq. 11) likewise MAPG, i.e.,

$$r^m = \prod_i \frac{\pi^i(a^i | \tau^i)}{\pi_{\text{old}}^i(a^i | \tau^i)} \quad (14)$$

$$J = \mathbb{E}_{a_t, s_t \sim \pi_{\text{old}}} \left[ \min \left( r^m A^{\text{old}}(s, a), \text{clip}(r^m, 1 - \epsilon, 1 + \epsilon) A^{\text{old}}(s, \vec{a}) \right) \right] \quad (15)$$

However, in practice, **such joint policy of product form may lead to numerical overflow and large variance with a large number of agents**. Therefore, we show a surrogate objective function that is suitable for multi-agent settings: since the KL-divergence is additive for independent distributions in much the same way as Shannon entropy; The KL-divergence constraint (Eq. 6) between the joint policy  $\pi_{\text{old}}$  and  $\pi$ ,

$$\mathbb{E}_{s \sim \rho^{\pi_{\text{old}}}} \left[ D_{\text{KL}} \left( \prod_i \pi_{\text{old}}^i(\cdot | s) \parallel \prod_i \pi^i(\cdot | s) \right) \right] \leq \delta. \quad (16)$$

can be simplified as <sup>1</sup>,

$$\mathbb{E}_{s \sim \rho^{\pi_{\text{old}}}} \left[ \sum_i D_{\text{KL}} \left( \pi_{\text{old}}^i(\cdot | s) \parallel \pi^i(\cdot | s) \right) \right] \leq \delta. \quad (17)$$

Therefore, we just need the following constraint for each agent  $i$  to hold,

$$\mathbb{E}_{s \sim \rho^{\pi_{\text{old}}}} \left[ D_{\text{KL}} \left( \pi_{\text{old}}^i(\cdot | \tau^i) \parallel \pi^i(\cdot | \tau^i) \right) \right] \leq \frac{\delta}{N} \quad (18)$$

Then, we consider the original objective functions,

<sup>1</sup>For the KL constraint, we assume that the sub-policies are independent.

$$\begin{aligned}
J^{MAPPO} &= \mathbb{E}_{\vec{a}_t, s_t \sim \pi_{\text{old}}} \left[ \frac{\pi(\vec{a}_t | s_t)}{\pi_{\text{old}}(\vec{a}_t | s_t)} A^{\text{old}}(s_t, \vec{a}_t) \right] \\
&\approx \mathbb{E}_{\vec{a}_t, s_t \sim \pi_{\text{old}}} \left[ \prod_i \frac{\pi^i(a_t^i | s_t^i)}{\pi_{\text{old}}^i(a_t^i | s_t^i)} A^{\text{old}}(s_t, \vec{a}_t) \right] \\
&\approx \mathbb{E}_{\vec{a}_t, s_t \sim \pi_{\text{old}}} \left[ \prod_i \frac{\pi^i(a_t^i | \tau_t^i)}{\pi_{\text{old}}^i(a_t^i | \tau_t^i)} A^{\text{old}}(s_t, \vec{a}_t) \right]
\end{aligned} \quad (19)$$

and our surrogate objective functions,

$$\begin{aligned}
\widehat{J^{MAPPO}} &= \mathbb{E}_{\vec{a}_t, s_t \sim \pi_{\text{old}}} \left[ \frac{1}{N} \sum_i \frac{\pi^i(a_t^i | s_t^i)}{\pi_{\text{old}}^i(a_t^i | s_t^i)} A^{\text{old}}(s_t, \vec{a}_t) \right] \\
&\approx \frac{1}{N} \sum_i \mathbb{E}_{\vec{a}_t, s_t \sim \pi_{\text{old}}} \left[ \frac{\pi^i(a_t^i | \tau_t^i)}{\pi_{\text{old}}^i(a_t^i | \tau_t^i)} A^{\text{old}}(s_t, \vec{a}_t) \right]
\end{aligned} \quad (20)$$

We prove that

$$\text{maximize } \widehat{J^{MAPPO}} \Rightarrow \text{maximize } J^{MAPPO} \quad (21)$$

holds approximately in Appendix A. Intuitively, maximizing the size of item  $\frac{\pi^i(a_t^i | s_t^i)}{\pi_{\text{old}}^i(a_t^i | s_t^i)} A^{\text{old}}(s_t, \vec{a}_t)$  for each agent  $i \in N$  will also maximize the size of item  $\frac{\prod_i \pi^i(a_t^i | s_t^i)}{\prod_i \pi_{\text{old}}^i(a_t^i | s_t^i)} A^{\text{old}}(s_t, \vec{a}_t)$ .

The surrogate objective function (Eq. 20 and Eq. 18) has a better scalability and lower variance than that of the original objective function. Then, we can use the PPO to optimize the independent policies of the agents with observations  $o^i$ , called vanilla **Multi-agent PPO (MAPPO)**,

$$r^i = \frac{\pi^i(a^i | \tau^i)}{\pi_{\text{old}}^i(a^i | \tau^i)} \quad (22)$$

$$\begin{aligned}
J^{MAPPO2} &= \\
&\frac{1}{N} \sum_i \mathbb{E}_{\vec{a}_t, s_t \sim \pi_{\text{old}}} \left[ \min \left( r^i A^{\text{old}}, \text{clip}(r^i, 1 - \epsilon, 1 + \epsilon) A^{\text{old}} \right) \right]
\end{aligned} \quad (23)$$

Our analysis shows that the vanilla MAPPO is approximately equivalent to optimizing a multi-agent joint policy with PPO. These simplified objective functions (Eq. 12 and Eq. 23) with a shared advantage value function make vanilla MAPPO and MAPG more scalable as well as easy to implement. Since there is no monotonicity constraint in the actor-critic methods, the expressiveness of vanilla MAPPO and MAPG is not limited. Besides, thanks to the architecture without a value mixing network, vanilla MAPPO and MAPG also do not have the problem of exploding the number of  $Q_i$  in QMIX.

## 4 METHOD

### 4.1 Motivation

In the previous section, we obtained the surrogate objective function of MAPPO and MAPG with a centralized advantage function (or value function). Thus we can obtain the expected policy gradient for an agent  $i \in N$ ,

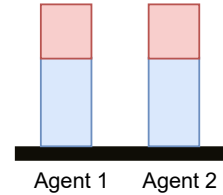
$$\frac{\partial \hat{J}}{\partial \pi^i(a_t^i | s_t)} \propto \mathbb{E}_{\vec{a}^{\neq i} \sim \pi} [A^\pi(s_t, a_t^i, \vec{a}^{\neq i})] \quad (24)$$

which can be seen as an implicit multi-agent credit [5, 23, 28] for agent  $i$ . According to the large number law, we need a large number of samples with the state  $s$  to estimate this expected gradient accurately. However, when the number of agents  $N$  is large, **it is almost impossible for us to traverse the action space of all the agents in a batch of samples** to obtain the true gradient. Therefore, in practice, we can usually only obtain the sampled mean gradient with deviations and large variance. These deviations may cause the policy of agent  $i$  to be updated in a sub-optimal direction, preventing the exploration of trajectories with higher returns. We call this problem: **The Policies Overfitting in Multi-agent Cooperation(POMAC)**.

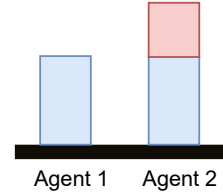
To explain this problem more straightforwardly, we consider a multi-agent cooperative task with two agents. We assume that there is only one sample with reward  $r_t$  in a batch, and the advantage value

$$A^\pi(s_t, \vec{a}_t) := r_t + \gamma V^\pi(s_{t+1}) - V^\pi(s_t) \quad (25)$$

is obtained by agent two and is not related to agent one<sup>2</sup>. The stochastic policy gradients with this shared advantage value, i.e.  $\frac{\partial \hat{J}}{\partial \pi^i(a_t^i | s_t)} \propto A^\pi(s_t, \vec{a}_t)$ , may improve probabilities of the policies of both agents, shown in Figure 1a. But intuitively, the agent one's policy should not be updated as the advantage value is not related to agent one, shown in Figure 1b.



(a) The stochastic policy gradient with the sampled shared advantage values.



(b) The true policy gradient.

**Figure 1: These bar charts represent the action probability, and the red area indicates the amount of improvement of the probability by the policy gradient.**

<sup>2</sup>For example, agent one and agent two are far apart and agent two gets a reward  $r_t$ .

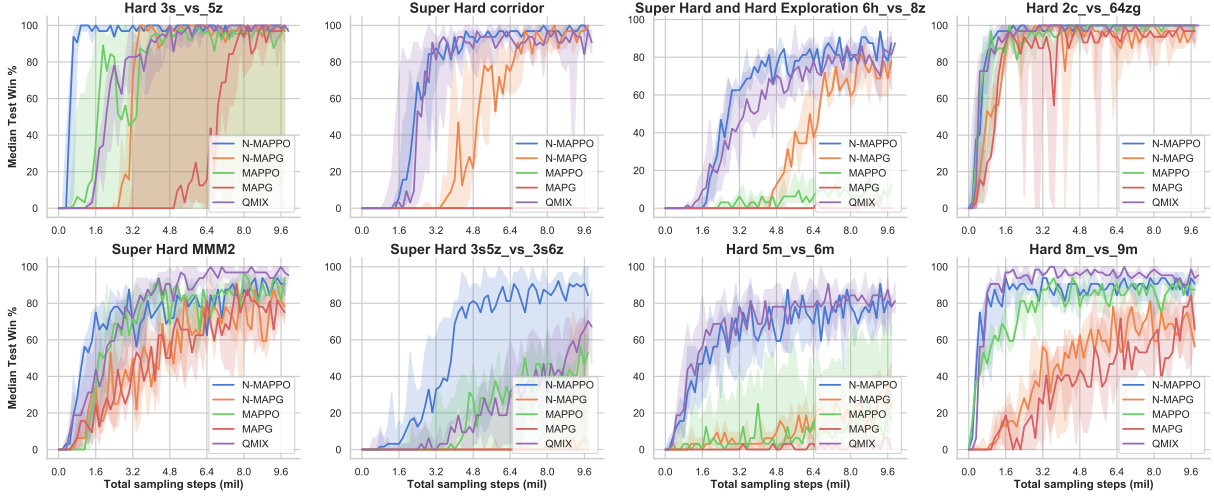


Figure 2: Median test win rate of MARL algorithms on hard scenarios in SMAC. N-MAPPO and N-MAPG denote Noisy-MAPPO and Noisy-MAPG.

## 4.2 Noisy Advantage Values

Inspired by the label smoothing technique [22, 31], we propose the noisy advantage values to solve this problem. For the first explicit noise method, i.e., Advantage-Noisy-MAPPO (ADV-N-MAPPO), demonstrated in Algo. 1. We randomly sample gaussian noise

$$x_b^i \sim \mathcal{N}(0, 1), \forall i \in N, b \in B \quad (26)$$

where  $B$  is the number of samples in a batch. Next, we mix the advantage values  $A^i$  with these noises by a weight  $\alpha$  (Eq. 27), perturbing the advantage values.

$$A_b^i = (1 - \alpha) \cdot A_b + \alpha \cdot x_b^i, \forall i \in N, b \in B \quad (27)$$

The noise of advantage values can be considered as a regularization technique that smooths out the sampled advantage values, likewise label smoothing [22, 31]. Thus the noise advantage values prevent the policies over-fitting and encourage multi-agent policies to explore diverse trajectories. However, the sharp signals of the explicit noise may destroy the original direction of the policy gradient. We then propose the second implicit noise method, i.e., Noisy Value-function. We randomly sample gaussian noise vectors  $\vec{x}^i \sim \mathcal{N}(0, \sigma^2)$ , where  $N$  is the number of agents and  $\sigma^2$  is the variance can be seen as the noise intensity. We concatenate the noise  $\vec{x}^i$  with state  $s$ . Next, we feed the concatenated feature to the centralized value network to generate noise value  $v^i$  for each agent  $i$ ,

$$v^i = V(\text{concat}(s, \vec{x}^i)), \forall i \in N \quad (28)$$

The random noise  $\vec{x}^i$  becomes moderated by the smoothing of the value neural networks. Then, the noise values  $v^i$  propagate to the advantage value  $A^i = r + \gamma v^i(s_t) - v^i(s_{t+1})$  for each agent, perturbing the advantage values. We then combine the Noisy Value function with MAPPO and MAPG to propose Noisy-MAPPO (N-MAPPO) and Noisy-MAPG (N-MAPG), demonstrated in Algo. 2

(Appendix B). We compare the performance of the two methods in the experimental section (Sec. 5.2.2).

## 5 EXPERINMENTS

In this section, we first evaluate the performance of (Advantage) Noisy-MAPPO and Noisy-MAPG in SMAC; and analyze how these noises affect their performance and the entropy of the policies of MAPPO. We then evaluate the expressive power of Noisy-MAPPO on two non-monotonic matrix games.

### 5.1 Benchmark Environments

**5.1.1 Starcraft Multi-agent Challenge (SMAC).** [24] focuses on micromanagement challenges where each unit is controlled by an independent agent that must act based on local observations, which has become a common-used benchmark for evaluating state-of-the-art MARL approaches, such as [5, 17, 23, 27]. SMAC offers diverse sets of scenarios, which are classified as Easy, Hard, and Super Hard scenarios. We use the hardest scenarios in SMAC as our main benchmark environment.

**5.1.2 Non-monotonic Matrix Game.** [27] [17] show the non-monotonic matrix games that violates the monotonicity constraint. For the matrix game Table 1a (Sec. 5.3); in order to obtain the reward 8, both agents must select the first action 0 (actions are indexed from top to bottom, left to right); if only one agent selects action 0, they obtain reward -12. QMIX learns incorrect  $Q_{tot}$  in such non-monotonic matrix games [27] [17]. We use two payoff matrices (Sec. 5.3, Table 1a and 1b) to evaluate the expressive power of Noisy-MAPPO.

**5.1.3 Evaluation Metric.** Our primary evaluation metric is the function that maps the steps for the environment observed throughout the training to the median test-winning percentage/median test return of the evaluation. Just as in QMIX [23], we repeat each experiment with several independent training runs (five independent random experiments).

## 5.2 SMAC

In this section, we evaluate the performance of the algorithms on SMAC. We test our noisy value function on MAPG and MAPPO, i.e., Noisy-MAPG and Noisy-MAPPO, respectively, in SMAC. It is worth noting that we use the fine-tuned QMIX from [8] as the baseline, as it achieves SOTA performance in SMAC among the previous works; we do not compare Noisy-MAPPO with MADDPG as the past experiments [21, 34] shows that it do not perform well under SMAC.

**5.2.1 Performance Comparison.** The experimental results in Figure 2 demonstrate that (1) **The performance of Noisy-MAPPO and Noisy-MAPG significantly exceeds that of vanilla MAPPO and MAPG on most hard scenarios, such as 3s\_vs\_5z, corridor (97%), 6h\_vs\_8z (81%) and 3s5z\_vs\_3s6z (31%).** (2) Benefiting from the surrogate objective function of TRPO, the sample efficiency of Noisy-MAPPO significantly outperforms Noisy-MAPG in all test scenarios. (3) The performance of Noisy-MAPPO is better than the fine-tuned QMIX on some scenarios, such as 3s\_vs\_5z, 6h\_vs\_8z and 3s5z\_vs\_3s6z; in other scenarios, the performance is also comparable to the fine-tuned QMIX. We show all the evaluation results in Appendix C.1. **All these results indicate that the noisy value function work well in practical tasks.** Since we use fine-tuned QMIX [8] as the baseline, the median test-winning rates of QMIX are significantly better than the experimental results in the past literature [17, 23, 24, 32].

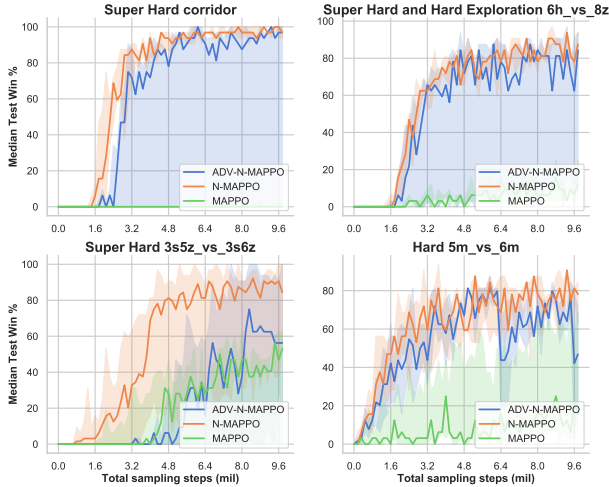


Figure 3: Comparing Noisy Advantage-value with Noisy Value-function.

**5.2.2 Comparing N-MAPPO with ADV-N-MAPPO.** We have proposed two noise-based methods (N-MAPPO and ADV-N-MAPPO) to resolve the POMAC problem in previous sections. In this section, we compare their performance in SMAC. As shown in Figure 3, we find that the Advantage-Noise method may harm the stability of the algorithm in some scenarios, such as 3s5z\_vs\_3s6z and 5m\_vs\_6m. We speculate that it may be the explicit noises destroy the original direction of the policy gradient. However, the performance of the Advantage-Noise method is still much better than that of vanilla

MAPPO in the Super Hard scenarios. All of these results indicate the noise advantage values does improve the performance of vanilla MAPPO.

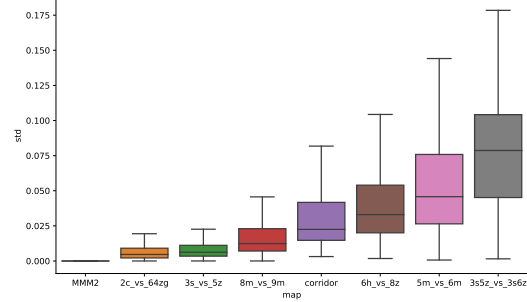


Figure 4: The standard deviation of value function  $v^i$  in the agent dimension.

The figure shows that scenarios with larger variance of  $v^i$  imply that noise also has a significant performance improvement on them.

**5.2.3 Variance of values  $v^i$ .** Next, we perform further experimental analysis on how the noisy value function affects the performance. We show the standard deviation of the value function  $v^i$  in agent dimension for some Hard scenarios in Figure 4. We find that **the large variance of  $v^i$  in some scenarios implies that the performance improvement of Noisy-MAPPO over vanilla MAPPO in these scenarios is also large**, such as 3s5z\_vs\_3s6z and 6h\_vs\_8z (see Figure 4 and Figure 3). This law reveals that the performance improvement of Noisy-MAPPO does come from noise perturbation of value function.

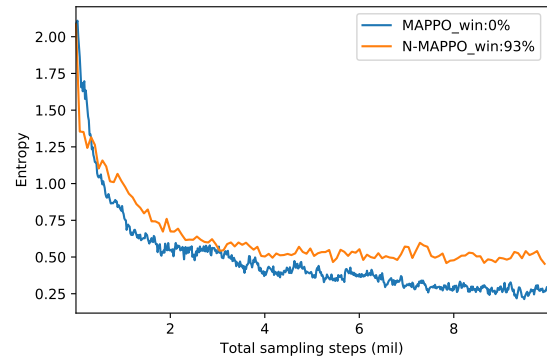


Figure 5: The average entropy of the policies of vanilla MAPPO and N-MAPPO.

**5.2.4 Policy entropy of MAPPO.** Finally we analyze the effect of the noise value function on the entropy of the policies on 6h\_vs\_8z. As shown in the Figure 5, because of POMAC problem, vanilla



MAPPO’s policy entropy drops rapidly and falls into the local optimal solution, and the winning rate is always zero. As for N-MAPPO, because we smoothed the shared advantage values, the policies are not easily overfitted and the policy entropy decreases more cautiously.

### 5.3 Non-monotonic Matrix Game

In this section, we evaluate the expressiveness of Noisy-MAPPO using two non-monotonic matrix games; As shown in Figure 6a and 6b, since there are no constraints on the value function of MAPPO (e.g., monotonicity constraints), the test performance of Noisy-MAPPO in both of these non-monotonic games are significantly better than QMIX. Since we use the fine-tuned QMIX, the test returns of QMIX in matrix 1b is better than that in the past literature [17].

8	-12	-12
-12	0	0
-12	0	0

(a) Payoff matrix 1

12	0	10
0	10	10
10	10	10

(b) Payoff matrix 2

Table 1: Non-monotonic matrix games from [27] (a) and [17](b)

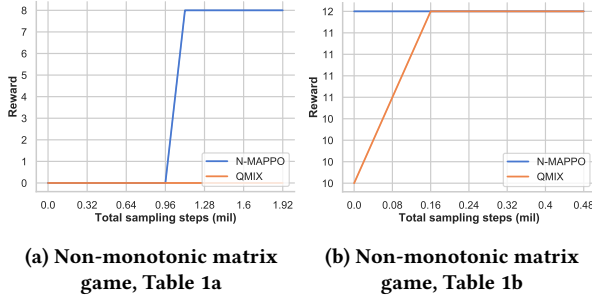


Figure 6: Test returns for non-monotonic matrix games from Sec.5.3

## 6 RELATED WORKS

In this section we connect our work to previous works, such as MAPPO-agent-specific [33], multi-agent Trust Region Policy Optimization (TRPO) [14], policy regularization and Noisy-Nets [6].

**MAPPO-agent-specific** [33] finetunes the hyperparameters of PPO to enable it to perform well in complex multi-agent tasks such as SMAC. We called it MAPPO-agent-specific (MAPPO-AS) as it feeds expert artificial features (agent-specific features) to the value networks, which significantly improved MAPPO’s performance in SMAC. The agent-specific features concatenate the global state  $s$  with agent-specific information, such as agent actions mask and agent’s own information. However, [33] does not give a theoretical analysis about the convergence of MAPPO and its working mechanism. At last, we make a comparison of the performance

of MAPPO-AS and Noisy-MAPPO in the Appendix C.1, and the results show that our random noise method outperforms it without artificial agent-specific features. Table 2 shows the difference between our method and MAPPO-AS in detail.

Algo.	MAPPO-AS	Noisy-MAPPO
Expert features	Yes	No
Centralized Value-function	No	Yes
Noise	No	Yes
Theoretical support	No	Yes

Table 2: The difference between MAPPO-AS and Noisy-MAPPO.

**multi-agent TRPO** Recently, [14] propose a multi-agent TRPO algorithm. However, this algorithm can only optimize decentralized policies based on local observations and **private rewards** for each agent, which may not be suitable for complex cooperative tasks with shared rewards. Our method only needs the shared reward without credit assignment.

**Policy-Regularization** A lot of works have been done to study policy regularization in reinforcement learning, e.g. the Soft Q-learning [30] and Soft Actor-Critic [7] propose the maximum entropy policies, which significantly improve the performance and stability of reinforcement learning algorithm. Munchausen Reinforcement Learning [7] adds the scaled log-policy to the immediate reward, which can be considered as it implicitly performs Kullback-Leibler (KL) regularization between consecutive policies. Our proposed noisy advantage values can also be considered as a policy regularization method and play an important role in some hard MARL scenarios.

**Noisy-Nets** [6] To improve the exploration in single-agent RL algorithms, [6] proposes the Noisy Neural Networks (Noisy-Nets) whose weights and biases are perturbed by a parametric function of the noise. These parameters are adapted with gradient descent. Consider a linear layer of a neural network,

$$y \stackrel{\text{def}}{=} (\mu^w + \sigma^w \odot \varepsilon^w) x + \mu^b + \sigma^b \odot \varepsilon^b \quad (29)$$

where  $\mu^w + \sigma^w \odot \varepsilon^w$  and  $\mu^b + \sigma^b \odot \varepsilon^b$  replace the weight and bias in linear layer, and  $\varepsilon$  is the random noise. Then they use Noisy-Nets as the last layer of the Deep-Q networks (DQN)[19] to enhance its exploration. By contrast, our work only to perturbs the input layer of the value network for each episode sample by a set of random noise.

## 7 CONCLUSION

In this paper, we extend the single-agent PG and PPO algorithms to MAPG and MAPPO algorithms with a theoretical support. Then, to solve the POMAC problem in MAPG and vanilla MAPPO, we propose two noisy advantage-value methods (N-MAPPO and ADV-N-MAPPO). The experimental results show that Noisy-MAPPO achieves more than 90% win rate in the most scenarios of SMAC without limitation of expressiveness and scalability. Our work demonstrates that the regularization of policies with noisy advantage values effectively improve the performance of the Multi-agent Actor-Critic algorithms.

## REFERENCES

- [1] Christopher Berner, Greg Brockman, Brooke Chan, Vicki Cheung, Przemyslaw Dębiak, Christy Dennison, David Farhi, Quirin Fischer, Shariq Hashme, Chris Hesse, et al. 2019. Dota 2 with large scale deep reinforcement learning. *arXiv preprint arXiv:1912.06680* (2019).
- [2] Yongcan Cao, Wenwu Yu, Wei Ren, and Guanrong Chen. 2012. An overview of recent progress in the study of distributed multi-agent coordination. *IEEE Transactions on Industrial Informatics* 9, 1 (2012), 427–438.
- [3] Yu-Han Chang, Tracey Ho, and Leslie P Kaelbling. 2004. All learning is local: Multi-agent learning in global reward games. (2004).
- [4] Christian Schroeder de Witt, Tarun Gupta, Denys Makoviichuk, Viktor Makoviichuk, Philip HS Torr, Mingfei Sun, and Shimon Whiteson. 2020. Is Independent Learning All You Need in the StarCraft Multi-Agent Challenge? *arXiv preprint arXiv:2011.09533* (2020).
- [5] Jakob N. Foerster, Gregory Farquhar, Triantafyllos Afouras, Nantas Nardelli, and Shimon Whiteson. 2018. Counterfactual Multi-Agent Policy Gradients. In *Proceedings of the Thirty-Second AAAI Conference on Artificial Intelligence (AAAI-18), the 30th innovative Applications of Artificial Intelligence (IAAI-18), and the 8th AAAI Symposium on Educational Advances in Artificial Intelligence (EAAI-18), New Orleans, Louisiana, USA, February 2-7, 2018*, Sheila A. McIlraith and Kilian Q. Weinberger (Eds.). AAAI Press, 2974–2982. <https://www.aaai.org/ocs/index.php/AAAI/AAAI18/paper/view/17193>
- [6] Meire Fortunato, Mohammad Gheshlaghi Azar, Bilal Piot, Jacob Menick, Ian Osband, Alex Graves, Vlad Mnih, Remi Munos, Demis Hassabis, Olivier Pietquin, et al. 2017. Noisy networks for exploration. *arXiv preprint arXiv:1706.10295* (2017).
- [7] Tuomas Haarnoja, Aurick Zhou, Pieter Abbeel, and Sergey Levine. 2018. Soft actor-critic: Off-policy maximum entropy deep reinforcement learning with a stochastic actor. In *International conference on machine learning*. PMLR, 1861–1870.
- [8] Jian Hu, Siyang Jiang, Seth Austin Harding, Haibin Wu, and Shih-wei Liao. 2021. Rethinking the Implementation Tricks and Monotonicity Constraint in Cooperative Multi-Agent Reinforcement Learning. *arXiv preprint arXiv:2102.03479* (2021).
- [9] Maximilian Hüttenrauch, Adrian Sošić, and Gerhard Neumann. 2017. Guided deep reinforcement learning for swarm systems. *arXiv preprint arXiv:1709.06011* (2017).
- [10] Shariq Iqbal and Fei Sha. 2019. Actor-Attention-Critic for Multi-Agent Reinforcement Learning. In *Proceedings of the 36th International Conference on Machine Learning, ICML 2019, 9-15 June 2019, Long Beach, California, USA (Proceedings of Machine Learning Research, Vol. 97)*, Kamalika Chaudhuri and Ruslan Salakhutdinov (Eds.). PMLR, 2961–2970. <http://proceedings.mlr.press/v97/iqbal19a.html>
- [11] Sham M Kakade. 2001. A natural policy gradient. *Advances in neural information processing systems* 14 (2001).
- [12] Diederik P. Kingma and Jimmy Ba. 2015. Adam: A Method for Stochastic Optimization. In *3rd International Conference on Learning Representations, ICLR 2015, San Diego, CA, USA, May 7-9, 2015, Conference Track Proceedings*, Yoshua Bengio and Yann LeCun (Eds.). <http://arxiv.org/abs/1412.6980>
- [13] Landon Kraemer and Bikramjit Banerjee. 2016. Multi-Agent Reinforcement Learning as a Rehearsal for Decentralized Planning. *Neurocomputing* 190 (2016), 82–94. <https://doi.org/10.1016/j.neucom.2016.01.031>
- [14] Hepeng Li and Haibo He. 2020. Multi-Agent Trust Region Policy Optimization. *arXiv preprint arXiv:2010.07916* (2020).
- [15] Timothy P. Lillicrap, Jonathan J. Hunt, Alexander Pritzel, Nicolas Heess, Tom Erez, Yuval Tassa, David Silver, and Daan Wierstra. 2016. Continuous control with deep reinforcement learning. In *4th International Conference on Learning Representations, ICLR 2016, San Juan, Puerto Rico, May 2-4, 2016, Conference Track Proceedings*, Yoshua Bengio and Yann LeCun (Eds.). <http://arxiv.org/abs/1509.02971>
- [16] Ryan Lowe, Yi Wu, Aviv Tamar, Jean Harb, Pieter Abbeel, and Igor Mordatch. 2017. Multi-Agent Actor-Critic for Mixed Cooperative-Competitive Environments. In *Advances in Neural Information Processing Systems 30: Annual Conference on Neural Information Processing Systems 2017, December 4-9, 2017, Long Beach, CA, USA*, Isabelle Guyon, Ulrike von Luxburg, Samy Bengio, Hanna M. Wallach, Rob Fergus, S. V. N. Vishwanathan, and Roman Garnett (Eds.), 6379–6390. <https://proceedings.neurips.cc/paper/2017/hash/68a9750337a418a86fe06c1991a1d64c-Abstract.html>
- [17] Anuj Mahajan, Tabish Rashid, Mikayel Samvelyan, and Shimon Whiteson. 2019. MAVEN: Multi-Agent Variational Exploration. In *Advances in Neural Information Processing Systems 32: Annual Conference on Neural Information Processing Systems 2019, NeurIPS 2019, December 8-14, 2019, Vancouver, BC, Canada*, Hanna M. Wallach, Hugo Larochelle, Alina Beygelzimer, Florence d’Alché-Buc, Emily B. Fox, and Roman Garnett (Eds.), 7611–7622. <https://proceedings.neurips.cc/paper/2019/hash/f816dc0acf67498e10496222e9db10-Abstract.html>
- [18] Volodymyr Mnih, Adrià Puigdomènech Badia, Mehdi Mirza, Alex Graves, Timothy P. Lillicrap, Tim Harley, David Silver, and Koray Kavukcuoglu. 2016. Asynchronous Methods for Deep Reinforcement Learning. In *Proceedings of the 33rd International Conference on Machine Learning, ICML 2016, New York City, NY, USA, June 19-24, 2016 (JMLR Workshop and Conference Proceedings, Vol. 48)*, Maria-Florina Balcan and Kilian Q. Weinberger (Eds.). JMLR.org, 1928–1937. <http://proceedings.mlr.press/v48/mniha16.html>
- [19] Volodymyr Mnih, Koray Kavukcuoglu, David Silver, Alex Graves, Ioannis Antonoglou, Daan Wierstra, and Martin Riedmiller. 2013. Playing atari with deep reinforcement learning. *arXiv preprint arXiv:1312.5602* (2013).
- [20] Sylvie CW Ong, Shao Wei Png, David Hsu, and Wee Sun Lee. 2009. POMDPs for robotic tasks with mixed observability. 5 (2009), 4.
- [21] Bei Peng, Tabish Rashid, Christian A Schroeder de Witt, Pierre-Alexandre Kamieny, Philip HS Torr, Wendelin Böhmer, and Shimon Whiteson. 2020. FACMAC: Factored Multi-Agent Centralised Policy Gradients. *arXiv e-prints* (2020), arXiv–2003.
- [22] Gabriel Pereyra, George Tucker, Jan Chorowski, Łukasz Kaiser, and Geoffrey Hinton. 2017. Regularizing neural networks by penalizing confident output distributions. *arXiv preprint arXiv:1701.06548* (2017).
- [23] Tabish Rashid, Mikayel Samvelyan, Christian Schröder de Witt, Gregory Farquhar, Jakob N. Foerster, and Shimon Whiteson. 2018. QMIX: Monotonic Value Function Factorisation for Deep Multi-Agent Reinforcement Learning. In *Proceedings of the 35th International Conference on Machine Learning, ICML 2018, Stockholm, Sweden, July 10-15, 2018 (Proceedings of Machine Learning Research, Vol. 80)*, Jennifer G. Dy and Andreas Krause (Eds.). PMLR, 4292–4301. <http://proceedings.mlr.press/v80/rashid18a.html>
- [24] Mikayel Samvelyan, Tabish Rashid, Christian Schroeder de Witt, Gregory Farquhar, Nantas Nardelli, Tim G. J. Rudner, Chia-Man Hung, Philip H. S. Torr, Jakob Foerster, and Shimon Whiteson. 2019. The StarCraft Multi-Agent Challenge. *arXiv preprint arXiv:1902.04043* (2019).
- [25] John Schulman, Sergey Levine, Pieter Abbeel, Michael Jordan, and Philipp Moritz. 2015. Trust region policy optimization. In *International conference on machine learning*. PMLR, 1889–1897.
- [26] John Schulman, Filip Wolski, Prafulla Dhariwal, Alec Radford, and Oleg Klimov. 2017. Proximal policy optimization algorithms. *arXiv preprint arXiv:1707.06347* (2017).
- [27] Kyunghwan Son, Daewoo Kim, Wan Ju Kang, David Hostallero, and Yung Yi. 2019. QTRAN: Learning to Factorize with Transformation for Cooperative Multi-Agent Reinforcement Learning. In *Proceedings of the 36th International Conference on Machine Learning, ICML 2019, 9-15 June 2019, Long Beach, California, USA (Proceedings of Machine Learning Research, Vol. 97)*, Kamalika Chaudhuri and Ruslan Salakhutdinov (Eds.). PMLR, 5887–5896. <http://proceedings.mlr.press/v97/son19a.html>
- [28] Peter Sunehag, Guy Lever, Audrunas Gruslys, Wojciech Marian Czarnecki, Vinicius Zambaldi, Max Jaderberg, Marc Lanctot, Nicolas Sonnerat, Joel Z. Leibo, Karl Tuyls, and Thore Graepel. 2017. Value-Decomposition Networks For Cooperative Multi-Agent Learning. *arXiv preprint arXiv:1706.05296* (2017).
- [29] Ming Tan. 1993. Multi-agent reinforcement learning: Independent vs. cooperative agents. In *Proceedings of the tenth international conference on machine learning*. 330–337.
- [30] Ermo Wei, Drew Wicke, David Freelan, and Sean Luke. 2018. Multiagent Soft Q-Learning. *arXiv preprint arXiv:1804.09817* (2018).
- [31] Qizhe Xie, Minh-Thang Luong, Eduard Hovy, and Quoc V Le. 2020. Self-training with noisy student improves imagenet classification. In *Proceedings of the IEEE/CVF Conference on Computer Vision and Pattern Recognition*. 10687–10698.
- [32] Yaodong Yang, Jianye Hao, Ben Liao, Kun Shao, Guangyong Chen, Wulong Liu, and Hongyao Tang. 2020. Qatten: A General Framework for Cooperative Multiagent Reinforcement Learning. *arXiv preprint arXiv:2002.03939* (2020).
- [33] Chao Yu, Akash Velu, Eugene Vinitzky, Yu Wang, Alexandre Bayen, and Yi Wu. 2021. The surprising effectiveness of mapo in cooperative, multi-agent games. *arXiv preprint arXiv:2103.01955* (2021).
- [34] Meng Zhou, Ziyu Liu, Pengwei Sui, Yixuan Li, and Yuk Ying Chung. 2020. Learning Implicit Credit Assignment for Multi-Agent Actor-Critic. *arXiv preprint arXiv:2007.02529* (2020).



## A PROOF

Definition A.1. Original objective function:

$$\begin{aligned} J^{\hat{MAPPO}} &= \mathbb{E}_{\tau \sim \mathcal{D}} \left[ \frac{\pi(\vec{a}_t | s_t)}{\pi_{\text{old}}(\vec{a}_t | s_t)} A_t^{\text{old}}(s_t, \vec{a}^t) \right] \\ &= \mathbb{E}_{\tau \sim \mathcal{D}} \left[ \prod_i \frac{\pi^i(a_t^i | s_t)}{\pi_{\text{old}}^i(a_t^i | s_t)} A_t^{\text{old}}(s_t, \vec{a}^t) \right] \end{aligned}$$

Surrogate objective function:

$$\widehat{J^{\hat{MAPPO}}} = \mathbb{E}_{\tau \sim \mathcal{D}} \left[ \frac{1}{N} \sum_i \frac{\pi^i(a_t^i | s_t)}{\pi_{\text{old}}^i(a_t^i | s_t)} A_t^{\text{old}}(s_t, \vec{a}^t) \right]$$

where  $\mathcal{D}$  is the trajectories sampled by joint policy  $\pi^{\text{old}}$ ; and  $N$  is the number of agents.

In this section, we prove that

$$\text{maximize } \widehat{J^{\hat{MAPPO}}} \Rightarrow \text{maximize } J^{\hat{MAPPO}} \quad (30)$$

holds approximately with following **constraints**,

- (1) Clip constraint:  $1 - \epsilon \leq \frac{\pi^i(a_t^i | s_t)}{\pi_{\text{old}}^i(a_t^i | s_t)} \leq 1 + \epsilon$ , where  $\epsilon$  is the clip parameter.
- (2) Probability constraint:  $\sum_{k=1}^{|\mathcal{K}|} \pi^i(a_t^{i,k} | s_t) = 1$ , where  $\mathcal{K}$  denotes all actions of the agent.

PROOF. We know that that maximizing surrogate objective function  $\widehat{J^{\hat{MAPPO}}}$  is equivalent to,

- (1) Maximizing the individual ratio for each agent  $\frac{\pi^i(a_t^i | s_t)}{\pi_{\text{old}}^i(a_t^i | s_t)}$  for each item in  $\widehat{J^{\hat{MAPPO}}}$  that  $A_t^{\text{old}} > 0$ .
- (2) Minimizing the individual ratio for each agent  $\frac{\pi^i(a_t^i | s_t)}{\pi_{\text{old}}^i(a_t^i | s_t)}$  for each item in  $\widehat{J^{\hat{MAPPO}}}$  that  $A_t^{\text{old}} < 0$ .

and maximizing original objective function  $J^{\hat{MAPPO}}$  is equivalent to,

- (1) Maximizing the joint ratio  $\prod_i \frac{\pi^i(a_t^i | s_t)}{\pi_{\text{old}}^i(a_t^i | s_t)}$  for each item in  $J^{\hat{MAPPO}}$  that  $A_t^{\text{old}} > 0$ .
- (2) Minimizing the joint ratio  $\prod_i \frac{\pi^i(a_t^i | s_t)}{\pi_{\text{old}}^i(a_t^i | s_t)}$  for each item in  $J^{\hat{MAPPO}}$  that  $A_t^{\text{old}} < 0$ .

Due to the probability constraint, the above problems can be equated as: **transferring the action probability of the items with small advantage value  $A^{\text{small}}$  to the items with large advantage value  $A^{\text{large}}$** .

Given that  $\pi^* = \arg \max_{\pi} \widehat{J^{\hat{MAPPO}}}$ , and there exists

$$\begin{aligned} \pi' &= \arg \max_{\pi} J^{\hat{MAPPO}} \neq \pi^* \text{ and} \\ J^{\hat{MAPPO}}_{\pi'} &> J^{\hat{MAPPO}}_{\pi^*} \end{aligned}$$

which means that there are some action probability transfers between  $\pi^*$  and  $\pi'$ : e.g, given a pair of items with the same state  $s$  and different actions  $\vec{a}$  and  $\vec{a}'$ , in the original objective function  $J^{\hat{MAPPO}}_{\pi^*}$ ,

$$\frac{\pi^{j,*}(a^j | s)}{\pi_{\text{old}}^j(a^j | s)} \cdot \prod_{i \neq j} \frac{\pi^{i,*}(a^i | s)}{\pi_{\text{old}}^i(a^i | s)} A^{\text{old}}(s, \vec{a}) \quad (31)$$

$$\frac{\pi^{j,*}(a^{j'} | s)}{\pi_{\text{old}}^j(a^{j'} | s)} \cdot \prod_{i \neq j} \frac{\pi^{i,*}(a^i | s)}{\pi_{\text{old}}^i(a^i | s)} A^{\text{old}}(s, \vec{a}') \quad (32)$$

$\pi'$  can transfer the action probability of  $\pi^{j,*}(a^{j'} | s)$  to  $\pi^{j,*}(a^j | s)$  to make that  $J^{\hat{MAPPO}}_{\pi'} > J^{\hat{MAPPO}}_{\pi^*}$  with following conditions hold for above two items,

- (1)  $\frac{A^{\text{old}}(s, \vec{a})}{\pi_{\text{old}}^j(a^j | s)} \prod_{i \neq j} \frac{\pi^{i,*}(a^i | s)}{\pi_{\text{old}}^i(a^i | s)} > \frac{A^{\text{old}}(s, \vec{a}')}{\pi_{\text{old}}^j(a^{j'} | s)} \prod_{i \neq j} \frac{\pi^{i,*}(a^i | s)}{\pi_{\text{old}}^i(a^i | s)}$ ; this allows the transfer of probabilities to increase the size of the sum of above a pair items.
- (2) Clip constraint:  $\frac{\pi^{j,*}(a^j | s)}{\pi_{\text{old}}^j(a^j | s)} < 1 + \epsilon$  and  $\frac{\pi^{j,*}(a^{j'} | s)}{\pi_{\text{old}}^j(a^{j'} | s)} > 1 - \epsilon$ .

As  $\pi^*$  is a optimal solution of  $\widehat{J^{\hat{MAPPO}}}_{\pi}$ , we obtain that

- (1)  $\frac{A^{\text{old}}(s, \vec{a})}{\pi_{\text{old}}^j(a^j | s)} \leq \frac{A^{\text{old}}(s, \vec{a}')}{\pi_{\text{old}}^j(a^{j'} | s)}$ ; if this inequality does not hold, we can obtain that  $\widehat{J^{\hat{MAPPO}}}_{\pi'} > \widehat{J^{\hat{MAPPO}}}_{\pi^*}$  with the action probability transfer from  $\pi^{j,*}(a^{j'} | s)$  to  $\pi^{j,*}(a^j | s)$ , which contradicts that  $\pi^*$  is the optimal solution of  $\widehat{J^{\hat{MAPPO}}}_{\pi}$ . As the  $A^{\text{old}}(s, \vec{a})$  determines the sign of the entire ratios items, this inequality implies that condition (1) can only hold if  $A^{\text{old}}(s, \vec{a})$  and  $A^{\text{old}}(s, \vec{a}')$  have the same sign. Thus the probability of the condition (1) holds is small.
- (2) By the previous equivalence problem of maximizing  $\widehat{J^{\hat{MAPPO}}}_{\pi}$ , we can see that most of the action probability ratios of  $\pi^*$  may approach the boundary of the Clip constraint with a small  $\epsilon$ . This implies that the probability of above condition (2) holds is small.

Thus we assume that above strict conditions hold with a small probability  $\eta$  for a ratio item  $\frac{\pi^{j,*}(a^j | s)}{\pi_{\text{old}}^j(a^j | s)}$  where  $j \in N$ . Then,  $\pi'$  can only transfer the actions probability of  $\eta \cdot |\mathcal{D}| \cdot N$  ratio items of  $J^{\hat{MAPPO}}_{\pi^*}$  to increase the size of it. Next, we obtained that

$$J^{\hat{MAPPO}}_{\pi'} - J^{\hat{MAPPO}}_{\pi^*} = \frac{\eta \cdot |\mathcal{D}| \cdot N \cdot C}{|\mathcal{D}|} = \eta NC \quad (33)$$

where  $C$  is the average lift size of  $J^{\hat{MAPPO}}_{\pi^*}$  for the action probability transfers; and  $C$  is a small value due to the Clip constraint. Finally, we can see that  $\pi^*$  is close to  $\pi'$  when the number of agents  $N$  is small.  $\square$

## B PSEUDOCODE

Algo. 2 and Algo. 1 demonstrate Noisy-MAPPO and Advantage-Noisy-MAPPO, respectively. Noisy-MAPPO adds Gaussian noise to the input layer of the Value Network, and Advantage-Noisy-MAPPO adds Gaussian noise directly to the normalized advantage values.

Senarios	Difficulty	N-MAPPO	vanilla MAPPO	MAPPO-AS	finetuned-QMIX
2s3z	Easy	<b>100%</b>	<b>100%</b>	<b>100%</b>	<b>100%</b>
1c3s5z	Easy	<b>100%</b>	<b>100%</b>	<b>100%</b>	<b>100%</b>
3s5z	Easy	<b>100%</b>	<b>100%</b>	<b>100%</b>	<b>100%</b>
2s_vs_1sc	Easy	<b>100%</b>	<b>100%</b>	<b>100%</b>	<b>100%</b>
3s_vs_5z	Hard	<b>100%</b>	98%	98%	<b>100%</b>
2c_vs_64zg	Hard	<b>100%</b>	<b>100%</b>	<b>100%</b>	<b>100%</b>
5m_vs_6m	Hard	<b>90%</b>	25%	75%	<b>90%</b>
8m_vs_9m	Hard	96%	93%	87%	<b>100%</b>
corridor	Super Hard	<b>100%</b>	3%	98%	<b>100%</b>
MMM2	Super Hard	96%	96%	93%	<b>100%</b>
3s5z_vs_3s6z	Super Hard	<b>87%</b>	56%	84%	75%(env=8)
6h_vs_8z	Super Hard	<b>96%</b>	15%	87%	91%
27m_vs_30m	Super Hard	<b>100%</b>	98%	93%	<b>100%</b>
Avg. Score	<b>Hard+</b>	<b>96.2%</b>	64.9%	90.6%	95.1%

Table 3: Median test win percentage of MARL algorithms in all scenarios; MAPPO-AS denotes MAPPO-agent-specific [33],

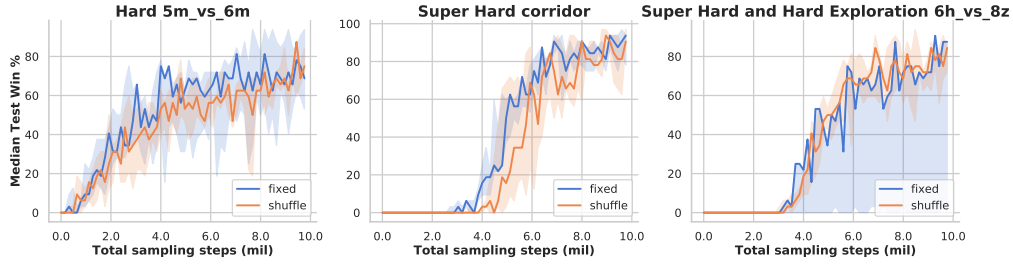


Figure 7: The performance comparison of fixed noise vectors and shuffle noise vectors (every 100 episodes).

## C EXPERIMENTAL DETAILS

### C.1 Experimental Results

Here, we echo the experiments in Sec. 5. Table 3 shows all experimental results for finetuned QMIX, vanilla MAPPO, Noisy-MAPPO (N-MAPPO), and MAPPO-agent-specific (MAPPO-AS). These test results show that the performance of Noisy-MAPPO is better than vanilla MAPPO and MAPPO-AS. In addition, the average performance of Noisy-MAPPO is better than that of QMIX.

### C.2 Hyperparameters

Our hyperparameters are heavily based on recent papers [33] and [8], who fine-tune PPO<sup>3</sup> and QMIX<sup>4</sup>, respectively, to make them work well in complex multi-agent tasks, such as SMAC. Table 4 shows the common hyperparameters of QMIX and MAPPO. Table 5 shows the hyperparameters of Noisy-MAPPO and Advantage-Noisy-MAPPO for each scenarios, where the values of  $\sigma$  are depend on the scenarios.

For the implementation of Noisy-MAPPO, **we do not shuffle the gaussian noise vectors  $x^i$  throughout the training**, as performance is comparable to non-shuffle version and easier to implement, as shown in Figure 7. Note that this fixed noise vector cannot be seen as an ID for an agent, as the value network cannot infer

that who you are just by the fixed noise vector  $\vec{x}$  and state  $s$  (unless you also feeds the observation  $o^i$ ).

**Other settings** We set the noise weight  $\alpha$  of Advantage-Noisy MAPPO to 0.05. For the non-monotonic matrix games, we set the number of environments of all algorithms to 32, buffer length to 1, noise vector dim to 10, training epochs to 10, and  $\sigma$  to 1. At last, we use StarCraft 2 (SC2.4.10) in the latest PyMARL in our experiments.

<sup>3</sup>PPO Code: <https://github.com/marlbenchmark/on-policy>

<sup>4</sup>QMIX code: <https://github.com/hijkzzz/pymarl2>

---

**Algorithm 1:** Advantage-Noisy-MAPPO

---

**input** : Initialize parameters  $\theta; \phi; \mathcal{D} \leftarrow \{\}$ ; batch size  $B$ ;  $N$  agents; noise weight  $\alpha$ ; entropy loss weight  $\eta$ ;  $\lambda$  for GAE( $\lambda$ );

1 **for** each episodic iteration **do**  
2   **for** episodic step  $t$  **do**  
3      $\vec{a}_t = [\pi_\theta^i(o_t^i), \forall i \in N]$ ;  
4     Execute actions  $\vec{a}_t$ , observe  $r_t, s_{t+1}, o_{t+1}$ ;  
5      $\mathcal{D} \leftarrow \mathcal{D} \cup \mathcal{D}\{(s_t, \vec{o}_t, \vec{a}_t, r_t, s_{t+1}, o_{t+1}, \cdot)\}$ ;  
6   **end**  
7   Sample random batch  $B$  from  $\mathcal{D}$ ;  
8   Compute advantage  $\hat{A}_1, \dots, \hat{A}_b$  and returns  $\hat{R}_1, \dots, \hat{R}_b$  via GAE( $\lambda$ );  
9   Sample Gaussian noise  $x_b^i \sim \mathcal{N}(0, 1), \forall i \in N, b \in B$ ; then mixing noise with advantage values:  
10      $\hat{A}_b^i = (1 - \alpha)\hat{A}_b + \alpha \cdot x_b^i, \forall i \in N, b \in B$   
11   **for** each training epochs **do**  
12     Update critic by minimizing the loss  $L(\phi)$ ;  
13     
$$L(\phi) = \frac{1}{B} \sum_{b=1}^B (v_b(\phi) - \hat{R}_b)^2$$
  
14     Update policy by using loss  $L(\theta)$ ;  
15     
$$r_b^i(\theta) = \frac{\pi_\theta^i(a_b^i | o_b^i)}{\pi_{\theta_{old}}^i(a_b^i | o_b^i)}, \forall i \in N, b \in B$$
  
16     
$$L(\theta) = \frac{1}{B \cdot N} \sum_{b=1}^B \sum_{i=1}^N [\min(r_b^i(\theta)\hat{A}_b^i, \text{clip}(r_b^i(\theta), 1 - \epsilon, 1 + \epsilon)\hat{A}_b^i) - \eta \mathcal{H}(\pi_\theta^i(o_b^i))]$$
  
17     where  $\mathcal{H}$  is the Shannon Entropy.  
18   **end**  
19 **end**

---

---

**Algorithm 2:** Noisy-MAPPO

---

**input** : Initialize parameters  $\theta; \phi; \mathcal{D} \leftarrow \{\}$ ; batch size  $B$ ;  $N$  agents; noise variance  $\sigma^2$ ; entropy loss weight  $\eta$ ;  $\lambda$  for GAE( $\lambda$ );

1 Sample random noise vectors  $\vec{x}^i$  for each agent,  $\vec{x}^i \sim \mathcal{N}(0, \sigma^2), \forall i \in N$ ;  
2 **for** each episodic iteration **do**  
3   **for** episodic step  $t$  **do**  
4      $\vec{a}_t = [\pi_\theta^i(o_t^i), \forall i \in N]$ ;  
5     Execute actions  $\vec{a}_t$ , observe  $r_t, s_{t+1}, o_{t+1}$ ;  
6      $\mathcal{D} \leftarrow \mathcal{D} \cup \mathcal{D}\{(s_t, \vec{o}_t, \vec{a}_t, r_t, s_{t+1}, o_{t+1}, \cdot)\}$ ;  
7   **end**  
8   **if** at noise vectors shuffle interval **then**  
9     Shuffle the noise vectors  $\vec{x}^i$  in agent dimension.  
10   **end**  
11   Sample random batch  $B$  from  $\mathcal{D}$ ;  
12   Noise value function forward for each agent,  $v_b^i(\phi) = V_\phi(\text{concat}(s_b, \vec{x}^i)), \forall i \in N, b \in B$ ;  
13   Compute advantage  $\hat{A}_1, \dots, \hat{A}_b$  and returns  $\hat{R}_1, \dots, \hat{R}_b$  via GAE( $\lambda$ ) with  $v_b^i(\phi), \forall i \in N, b \in B$ ;  
14   **for** each training epochs **do**  
15     Update critic by minimizing the loss  $L(\phi)$ ;  
16     
$$L(\phi) = \frac{1}{B \cdot N} \sum_{i=1}^B \sum_{i=1}^N (v_b^i(\phi) - \hat{R}_b^i)^2$$
  
17     Update policy by using loss  $L(\theta)$ ;  
18     
$$r_b^i(\theta) = \frac{\pi_\theta^i(a_b^i | o_b^i)}{\pi_{\theta_{old}}^i(a_b^i | o_b^i)}, \forall i \in N, b \in B$$
  
19     
$$L(\theta) = \frac{1}{B \cdot N} \sum_{b=1}^B \sum_{i=1}^N [\min(r_b^i(\theta)\hat{A}_b^i, \text{clip}(r_b^i(\theta), 1 - \epsilon, 1 + \epsilon)\hat{A}_b^i) - \eta \mathcal{H}(\pi_\theta^i(o_b^i))]$$
  
20     where  $\mathcal{H}$  is the Shannon Entropy.  
21   **end**  
22 **end**

---

hyperparameters	MAPPO/PG-based	QMIX
num envs	8	8
buffer length	400	-
batch size(episodes)	-	128
num GRU layers	1	1
RNN hidden state dim	64	64
fc layer dim	64	64
num fc before RNN	1	1
num fc after RNN	1	1
num noise dim	10	-
Adam [12] lr	5e-4	1e-3
activation	ReLU	ReLU
$Q(\lambda)$	-	0.6, (0.3 for 6h_vs_8z)
GAE( $\lambda$ )	0.95	-
entropy coef	0.01	-
PPO clip	0.2	-
noise shuffle interval	$+\infty$	-
$\epsilon$ anneal steps	-	100k, (500k for 6h_vs_8z)

**Table 4: Common hyperparameters used in the SMAC domain for all algorithms.**

map	epoch (for PPO-based)	mini-batch	gain	network	stacked frames	N-MAPPO	N-MAPG
						$\sigma$	$\sigma$
2s3z	15	1	0.01	rnn	1	1	1
1c3s5z	15	1	0.01	rnn	1	1	1
3s5z	5	1	0.01	rnn	1	1	1
2s_vs_1sc	15	1	0.01	rnn	1	1	1
3s_vs_5z	15	1	0.01	mlp	4	1	1
2c_vs_64zg	5	1	0.01	rnn	1	1	1
5m_vs_6m	10	1	0.01	rnn	1	8	3
8m_vs_9m	15	1	0.01	rnn	1	1	0
corridor	5	1	0.01	mlp	1	3	1
MMM2	5	2	1	rnn	1	0	0.5
3s5z_vs_3s6z	5	1	0.01	rnn	1	10	1
6h_vs_8z	5	1	0.01	mlp	1	1	1
27m_vs_30m	5	1	0.01	rnn	1	1	1

**Table 5: Hyperparameters for (Advantage) Noisy-MAPPO, Noisy-MAPG and MAPPO in SMAC.**